Design of a 4m Hopping Robot Using Off-the-Shelf Components

Josephus Driessen and Roy Featherstone
Dept. Advanced Robotics, Istituto Italiano di Tecnologia
via Morego 30, 16163 Genova, Italy

Abstract— **This paper describes a design process leading to a hopping robot able to reach a hopping height of 4 m using a standard, off-the-shelf electric motor and ball screw. The essence of the design process is as follows: the robot is made to operate (in simulation) at its performance limit by saturating the motor, the resulting motion is observed and compared with the desired motion, and the robot is redesigned so as to reduce the difference. The end result is a robot whose natural dynamics *at its performance envelope* coincides with the most demanding behaviour it is designed to deliver; and the role of feedback control is merely to fine-tune the behaviour rather than to try and impose an artificial dynamics on the robot. The design process is therefore holistic, as it considers the behaviour of the whole robot. It is also an example of machine and behaviour co-design, because only the final outcome (a 4 m hop) is specified in advance, not the action sequence to achieve it, and the objective is to discover both the robot and its behaviour.**

I. INTRODUCTION

Experimental legged robots, especially humanoids, exhibit levels of physical performance below what one would expect, given the capabilities of the technologies available to make them. One possible reason is that today's legged robots are so complex that a truly high-performance design of such a robot is simply too big a task for the relatively small teams of researchers who make them. To test this hypothesis, a project is under way to design, build and control a very simple 3D hopping and balancing robot, called Skippy, that will exhibit a level of physical performance substantially superior to today's legged robots [8], [9]. The ultimate objective of this project is to contribute to the improvement in the physical performance of legged robots in general by showing how such improvements can be obtained through a combination of better design and better control.

This paper focuses on the single most physically demanding item in Skippy's repertoire of behaviours: the stance phase prior to a 4 m hop. The stance phase is divided into a *landing phase*, in which the robot is flexing and the centre of mass (CoM) is going down, followed by a *launch phase*, in which the robot is extending and the CoM is going up. This paper focuses mainly on the launch phase, which is the phase with the greatest energy flows. Furthermore, as the motion takes place in the robot's saggital plane, and a separate balance controller ensures that this plane remains vertical, the problem will be simplified to that of a planar robot hopping in a vertical plane.

This paper is organized as follows. Section II compares Skippy to other high performance and hopping machines. Preliminary design decisions and principles of Skippy are summarized in Section III. The problem statement of the

design problem for achieving the 4 m hop is explained in Section IV. Section V then explains how our design strategy is applied to reach a 4 m high hop and presents the results. A conclusion is included in Section VI.

II. BACKGROUND

We pursue the design of a simple robot that exhibits high physical performance; in particular, jumping performance. Robots with similar principles and properties have been built successfully in the past. Usually, these robots employ one of two operating principles: *single-leap* robots charge an elastic element at a relatively slow rate, and then release it in a short burst, whereas *continuous-hopping* robots use an elastic element to recycle a portion of the kinetic energy of the previous hop into the next one. Skippy is a continuous-hopping robot.

The most notable work on continuous-hopping robots is Raibert's early work in the 1980s [19], which demonstrated several legged robots that could hop, run and make somersaults in 3D, while using simple designs and control systems. Their capabilities were deemed a large improvement in robotic physical performance for their time, and few machines have been able to equal or surpass their performance since.

Another example of a robot with high physical performance is MIT's quadrupedal Cheetah [21]. Although not designed as a jumping robot, it is able to achieve running gaits with high velocities of 6 m/s. (In comparison, Skippy must reach a vertical lift-off velocity of 9 m/s in order to make a 4 m high hop.) Both Skippy and Cheetah exploit their natural dynamics to realise these achievements. However, Skippy emphasizes maximizing the peak energy flow from the batteries to the mechanics in order to obtain the energy burst that is required to achieve its lift-off velocity in approximately half a stance phase (ca. 0.1 s), whereas the emphasis in Cheetah is on maximizing torque density, which enables it to eventually (i.e. over a longer time span) reach its high travelling velocity. Cheetah furthermore differs from Skippy in that it is bio-inspired, whereas Skippy is inspired from available technology.

Another example of a continuous-hopping robot is Festo's BionicKangaroo [11]. It is less athletic than Cheetah or Skippy, and has a maximum jumping height of 0.4 m.

Dynamic walkers are another class of robots that exploit natural dynamics. These robots are explicitly designed to achieve a specific behaviour, such as bipedal walking, typically derived from passive dynamic walking [16] or

spring-loaded inverted pendulum (SLIP) models [20], [22]. These machines have little or no actuation, so the focus is intrinsically more towards energy efficiency, which is associated with sacrifice of versatility and robustness.

Continuous-hopping robots have been able to reach jumping heights of approximately 0.6 m [12]. Single-leap robots have achieved much higher jumping heights. These robots include Boston Dynamics' wheeled SandFlea [7] and some bio-inspired robots using mechanical principles similar to those of a grasshopper. Sand Flea is able to jump up to at least 8 m high using a piston driven by a gas cylinder. The grasshopper robots, such as the EPFL Jumper [15], Glumper [1] and TAUB [26], are able to jump up to heights of 1.4 m, 1.6 m and 3.4 m, respectively, making use of a catapult mechanism where passive elements are slowly charged to accumulate jump energy. The EPFL Jumper and Glumper also have the ability to recover and reorient themselves after landing. A few robots combine jumping with another type of locomotion, such as the jumping-crawling robot JumpRoACH [13] and the jumping-gliding robot MultiMo-Bat [25], both able to jump up to heights of approximately 3 m.

III. PRELIMINARY DESIGN OF SKIPPY

Several design decisions have been made prior to the study presented in this paper, and those that are relevant are presented here. Figure 1(a) shows the current design of Skippy's mechanism. It is, essentially, a planar double pendulum with a crossbar at its head. The torso and leg together make a planar hopping and balancing machine, and the crossbar stabilizes and steers it in 3D. The feasibility of this behaviour was established in [3]–[5].

To facilitate the design study, we make two simplifications to this mechanism: (1) the crossbar is removed and its inertia added to the torso; and (2) the 4-bar linkage at the hip is replaced by a pair of revolute joints geared 1 : 1, as shown in Figure 1(b), which approximates the kinematics of the 4-bar linkage.

The robot's mass distribution is a compromise between the conflicting needs of hopping and balancing. For good hopping performance, the CoM must be as close as possible to the head; but for good balancing performance (as measured by velocity gain [10]) the torso needs a large radius of gyration. The compromise is to place most of the mass near the head, but have a small concentration of mass at the hip (i.e., the 4-bar linkage), and make the middle portion of the torso as light as possible. This is achieved by placing both the main motor and crossbar actuator close to the head. The main motor then drives the hip lever through a ball screw and the main spring.

The main spring is necessary for three reasons: to recycle energy from one hop to the next, to allow the main motor to do positive work during the landing phase as well as the launch phase, and to allow the hip joint to reach the necessary speed for lift-off.

The ankle spring also stores some energy, but the main purpose of the spring-loaded ankle is to allow the robot to control its angular momentum at lift-off. The operation of the ankle is illustrated in Figure 1(c), and can be explained as follows. First, the launch phase is divided into a *thrust phase*, during which the main motor is in saturation and the hip torque is high, followed by a *steering phase*, during which the main motor comes out of saturation and the hip torque is relatively low. At the beginning of the thrust phase (frame 1), the ankle joint is sitting at its flexion end-stop, and is held there by the high hip torque. This continues until the end of the thrust phase (frame 2); but then the reduced hip torque during the steering phase allows the ankle to extend (frame 3). Throughout the thrust phase, the ground reaction force (GRF) passes slightly to the right of the CoM, implying a build-up of positive angular momentum; but the change of motion as the ankle joint extends causes the GRF to change direction so that it passes to the left of the CoM. This offers the control system the possibility to bring the robot's net angular momentum to zero, or to a desired nonzero value, before lift-off.

A. Ballpark Figures

Skippy's target mass is 2 kg. At this mass, it requires 80 J of kinetic energy at lift-off to make a 4 m hop. It is a design requirement that Skippy be able to reach this height without relying on more than half of this energy being recycled from the previous hop. So the hip actuator must be able to supply at least 40 J of new kinetic energy during the stance phase. Assuming a stroke length of 0.45 m (the vertical component of CoM travel from its lowest point to lift-off), the stance phase will last approximately 0.2 s. This implies 9 g average vertical acceleration, 200 N average vertical GRF, and 200 W average power output from the hip actuator.

The limiting factor on the performance of this design is the maximum speed of the ball screw. In an earlier study [8], we selected an 8 mm diameter, 2 mm pitch ball screw with a thrust rating of 3 kN from the Steinmeyer catalog [23], paired with a Maxon RE35 90 W 24 V motor. However, upon discovering that this ball screw had been discontinued, we chose instead a 4 mm pitch model with a thrust rating of 2 kN, paired with a Maxon DCX32L 70 W 24 V motor which, despite the lower nominal power rating, can deliver substantially higher peak power than the original motor. The Steinmeyer ball screws can be operated at 6000 rpm,* which equates to a nut speed of 0.4 m/s. At this speed, the nut must pull at 500 N in order to deliver 200 W, and the necessary driving torque would be 0.35 Nm (assuming 90% efficiency). Two more limits are the 29.6 V available from the battery pack, which we round down to 29 V in the simulations in order to allow for voltage drops between the battery and the motor, and the 50 A current limit of the Pololu 24v21 motor drivers we are using [18]. Within these limits, the motor can deliver 0.97 Nm at 6000 rpm, and the maximum available output power is 633 W at 5062 rpm. The motor will overheat if Skippy makes a lengthy sequence of 4 m hops.

---

*Reported to us by colleagues in the robotics community. The catalog recommends a top speed of only 4500 rpm.
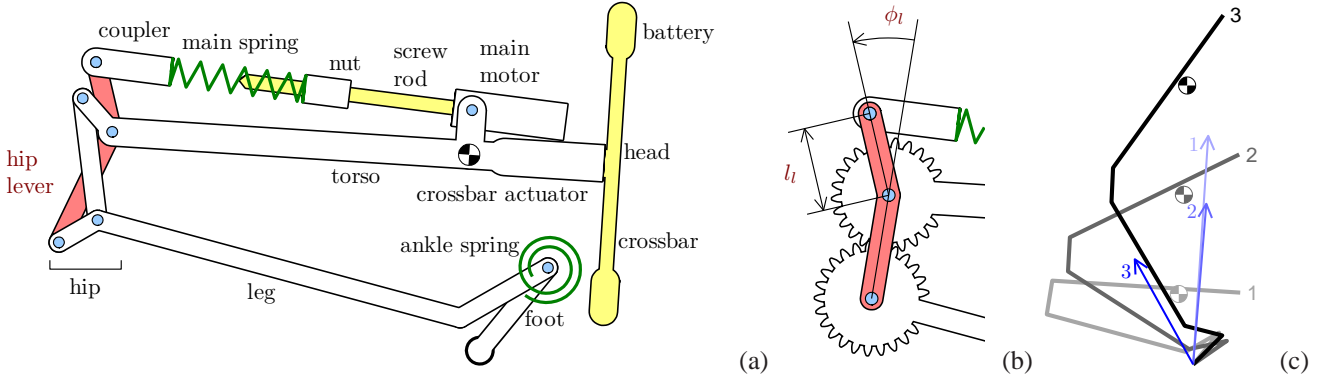
Fig. 1. (a) Skippy's mechanism, (b) replacing the 4-bar linkage with geared revolute joints, and (c) the function of the ankle joint during steering
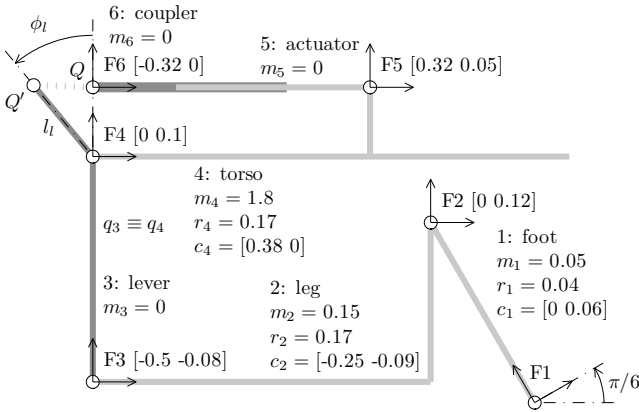

Fig. 2. Model of simplified Skippy mechanism in its zero position ($q = 0$). The diagram is not drawn to scale.

IV. PROBLEM STATEMENT

This paper covers only a small part of the design study of Skippy: the stance phase preceding a 4 m hop. Furthermore, the objective is only to demonstrate the achievability of a 4 m hop using the chosen motor and ball screw. We define a 4 m hop to be one in which the CoM reaches a height 4 m higher than its height at lift-off. We also require that the angular momentum at lift-off be zero.

The problem can be stated as follows. Given a realistic dynamic model of the simplified Skippy mechanism, find a suitable set of initial conditions, suitable values for certain model parameters, and a suitable control strategy, such that an accurate simulation shows that the robot has reached a sufficient velocity at lift-off to make a 4 m hop. The model parameters to be found are: the kinematic parameters l_l and ϕ_l of the hip lever, as shown in Figures 1(b) and 2, and the force profile of the main spring. All other parameters are given.

A. Model Parameters

The kinematic model and most inertia parameters are shown in Figure 2. Bodies and joints are numbered consecutively from a fixed base, and some bodies are also identified by name. Positive rotation of joint i causes counter-clockwise

rotation of body i relative to body $i - 1$. Joint 1 gives the overall orientation of the robot. The kinematic loop is shown open in the diagram, but the loop-closure constraint is enforced in the simulations (i.e. Q and Q' in Figure 2 coincide with each other). More details can be found in [8].

In place of the revolute joint between the motor's stator and rotor, and the helical joint between the screw rod and the nut, which are both out-of-plane motions, the rod, rotor and stator are treated as a single rigid body (body 5), and the coupler (body 6) is connected to this body via an actuated prismatic joint. The masses of these bodies, plus the nut, are modelled as being incorporated into the torso, which is justified by the fact that each body is either very light or moves very little with respect to the torso.

The actuator force is obtained from a detailed calculation that takes into account the extension and force profile of the main spring, the position and velocity of the nut on the rod, frictional loss in the ball screw, the rotational inertias of the rod and rotor, and the electrical and mechanical properties of the main motor [8].
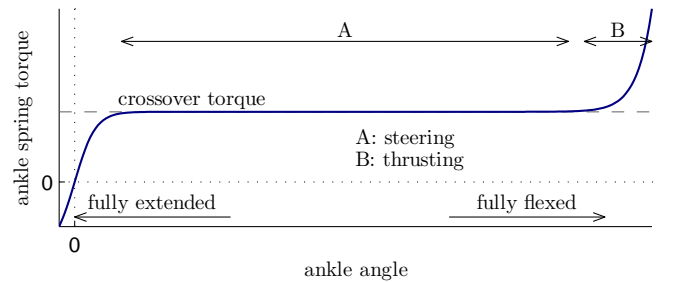

Fig. 3. Force profile of the ankle spring

The force profile of the ankle spring is plotted in Figure 3. This profile ensures that the ankle remains at its flexion end-stop throughout the thrust phase, but continues to press the foot firmly into the ground (to avoid slipping) during all but the final few milliseconds of the steering phase. The key parameter is the crossover torque, which is slightly lower than the lowest torque that the ankle must transmit during the thrust phase, and is set at 12 Nm.

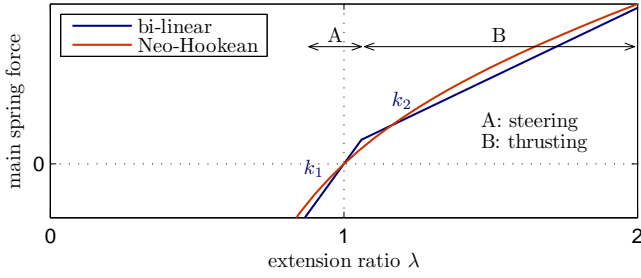The force profile of the main spring is plotted in Figure 4,

Fig. 4. Force profiles of the main spring: Neo-Hookean (new) and bilinear (old)

along with the bilinear profile used in earlier studies [8], which is included only for the sake of comparison. The profile needs to be regressive for the following reasons: (1) to maximize energy storage per unit extension at high force levels, and (2) to maximize stiffness at low force levels. The former helps Skippy to hop high with a limited actuator stroke, while the latter improves the actuator's bandwidth at low force levels, which increases the robot's ability to steer and to balance.

The new profile is that of a uni-axially loaded rubber (hyperelastic) cylinder modelled as a single Neo-Hookean element [24]. Rubber is chosen as the material of the main spring because of its very high gravimetric energy density (potential energy storage per unit of mass) [2]. The equation for this profile is

$$ F_{se} = C_0 \left(\lambda - \frac{1}{\lambda^2} \right) = C_0 \left(\frac{x_s}{x_0} - \frac{x_0^2}{x_s^2} \right) $$

where F_{se} is the elastic spring force, $\lambda = x_s/x_0$ the extension ratio, x_s the length of the rubber cylinder, x_0 the rest length and C_0 a constant proportional to the loaded surface area of the spring at rest. According to this equation, the stiffness at rest is $k_0 = 3C_0/x_0$, and approaches the limit $k_\infty = C_0/x_0$ as $\lambda \to \infty$. This equation is a reasonable approximation for rubber compression and strain up to approximately 50% ($\lambda = 1.5$) [24], after which the profile typically becomes slightly more regressive.
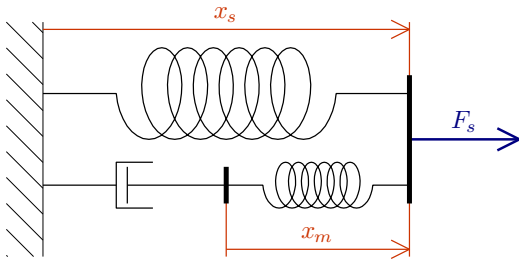

Fig. 5. Main spring model: an elastic non-linear spring in parallel with a Maxwell element (linear spring and damper in series).

To model the energy loss in the spring, one Maxwell element (a linear spring and damper in series) is connected in parallel with the neo-hookean element [6], [14], [17], see Figure 5. The force of the Maxwell element F_{sm} equals

$$ F_{sm} = (\dot{x}_s - \dot{x}_m) \, c_m = x_m k_m $$

with k_m the spring stiffness, c_m the damper viscosity and x_m the spring elongation. x_m is a state variable. The selected values of the Maxwell element parameters are $k_m = k_0/4$ and $c_m = k_m/60$. These values are chosen and scaled to match values found in the literature [6], corresponding to a type of rubber typically found in suspension components of rail vehicles. The total spring force, F_s, is then the sum of the elastic spring force, F_{se}, and the force exerted by the Maxwell element, F_{sm}.

This spring model has just two parameters: x_0 and C_0. In the next section, the desired initial conditions will place two constraints on the three quantities x_0, x_s and C_0; so we have one free parameter to choose now. As a high degree of regressiveness is desirable, and this is achieved by choosing a small value for x_0, we decided to set x_0 equal to twice the anticipated maximum extension of the spring (5 cm), this being the smallest value for x_0 that stays within the stated accuracy range of the above model ($\lambda \leq 1.5$). So $x_0 = 10$ cm.

V. Achieving the 4 m Hop

To achieve a 4 m hop, the main challenge is to move energy very quickly from the battery to the mechanism. Our strategy is therefore to focus on maximizing energy flow. This can be accomplished as follows.

1) Maximum energy flows from the battery to the main motor when the full battery voltage is applied to the motor. The motor is then said to be operating *in saturation*.
2) The motor's mechanical load must be designed such that when the motor is in saturation it is operating at a speed close to its maximum-power speed.
3) The mechanism, the springs and their initial conditions must be designed so as to convert as much as possible of the incoming mechanical power and stored elastic energy into vertical motion of the CoM.

As we are also interested in controllability, there is one more requirement:

4) The steering phase must be able to reach a range of possible angular momenta at lift-off, which must include zero.

We also need a control strategy for the hop. For the thrust phase this is easy: keep the motor in saturation. For the steering phase we chose to use bang-bang control on the grounds that it is simple and we found that it worked. We do not claim that it is optimal. For the landing phase, we found that it could be treated as an extension of the thrust phase. Again, we do not claim that this is optimal.

To facilitate the search for a solution, we first consider the launch phase in isolation, and then consider the stance phase as a whole. The reasoning behind this approach is that the launch phase contains the largest energy flows, and is therefore the phase most likely to be constrained by limiting factors.

A. Launch Phase

The launch phase begins when the CoM reaches its lowest point. To keep things simple, we assume that the robot mechanism's joint velocities are zero at this moment, but the motor velocity is not. With a supply voltage of $29\,\text{V}$, the motor's maximum-power speed is $\omega_{opt} = 5062\,\text{rpm}$, corresponding to a nut speed of $0.338\,\text{m/s}$. So our first decision is to set the motor speed to this value. The thrust force available at this speed, taking into account the losses in the ball screw, is $1.68\,\text{kN}$; so we set the initial tension on the main spring to this value. These choices ensures that the thrust phase begins at an optimal operating point, and we would like it to stay near this point during the whole of the thrust phase.

The state variable of the Maxwell element x_m is set to its steady state value for the initial velocity of the spring $\dot{x}_s$. The resulting initial energy storage in the Maxwell linear spring is $0.2\,\text{J}$.

In our first experiments, we set the total elastic energy stored in the two springs at the beginning of the launch phase to $65\,\text{J}$ calculated as follows: $40\,\text{J}$ of recycled kinetic energy from the previous hop, $10\,\text{J}$ from gravitational potential energy as the CoM drops from touch-down to its lowest point, plus $15\,\text{J}$ of new energy supplied by the main motor during the landing phase. However, we found by experiment that this figure is too high, and that a total elastic energy of $50\,\text{J}$ gives better results.

The initial elastic energy in the ankle spring can be calculated as $10\,\text{J}$ [8], from which it follows that the energy initially in the main spring must be $40\,\text{J}$. This requirement, plus the requirement that the initial tension be $1.68\,\text{kN}$, allows us to calculate $C_0 = 1786$ and the initial spring length $x_{s,0} = 14.32\,\text{cm}$.

Although the initial joint velocities can be assumed to be zero, a suitable initial configuration must be found by experiment. We found that the following configuration produces almost vertical hops: $q_{1,0} = -76.17°$, $q_{2,0} = 60°$, $q_{3,0} = q_{4,0} = 5°$, and other joints as determined by the loop-closure constraint. Many other configurations also work, resulting in different hop trajectories. Note that $q_{2,0}$ was decided at an earlier stage, when the ankle spring was being designed, and is therefore a given quantity. See [8] for details.

The two mechanism parameters to be tuned are the kinematic parameters l_l and ϕ_l of the hip lever shown in Figures 2 and 1(b). These have an influence on the value of the transmission ratio from the coupler to the leg, and its variation with hip angle, respectively. By manipulating ϕ_l, we can arrange for the hip motion to be forceful but relatively slow near maximum flexion, and fast but less forceful near maximum extension (close to the configuration at lift-off). However, there is a kinematic singularity that must be avoided. We found that an angle of $\phi_l = 10°$ gave good results.

Tuning the lever length is a trade-off between steering, thrust performance and heat generation. Shorter lever lengths allow the lever to reach higher angular velocities, increasing the steering performance. A shorter lever length also delays

nut acceleration during the thrust phase, which allows the motor to deliver close to maximum power for a longer time. On the other hand, a shorter lever length implies a higher motor torque, which in turn means a higher current draw, more joule heating of the motor windings and a lower motor efficiency. If the lever length is too short then the required torque is too far above the optimum-power torque, and Skippy becomes too feeble to make a $4\,\text{m}$ hop. A lever length of $l_l = 9\,\text{cm}$ was found to be a good compromise between these competing effects.

Figures 6 to 9 show the results of a launch phase with all of the above described system parameters and initial values, in which the motor is commanded to operate in saturation throughout the whole of the launch phase. This will be referred to as *maximum positive steering* on the grounds that it results in the most positive achievable angular momentum at lift-off. It also produces the highest hop. The resulting hopping height is $4.4\,\text{m}$.
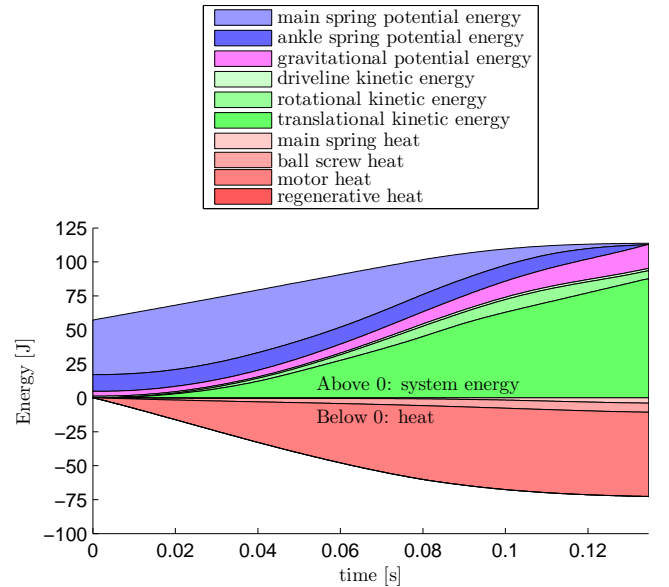

Fig. 6. The energy audit of Skippy's launch phase for maximum positive steering. It can be seen that most potential energy is converted to useful kinetic energy for hopping.

Figure 6 plots the values of all system energies and all energy losses as a function of time. The growth in total energy (including losses) should exactly match the energy drawn from the batteries. This is checked automatically in a process that we call an *energy audit*, which serves as a test of the correctness and accuracy of the simulation. The graph plots system energies above zero and energy losses, which are all labelled as 'heat', below zero. The item 'regenerative heat' refers to energy that flows from the mechanical system back into the motor, which is lost because our motor driver circuits do not support regeneration (motor acting as dynamo). Translational kinetic energy is defined as $\frac{1}{2}mv_{\text{cm}}^2$, where m is the mass of the robot and v_{cm} is the speed of the CoM. Rotational kinetic energy is total kinetic energy minus the translational kinetic energy.
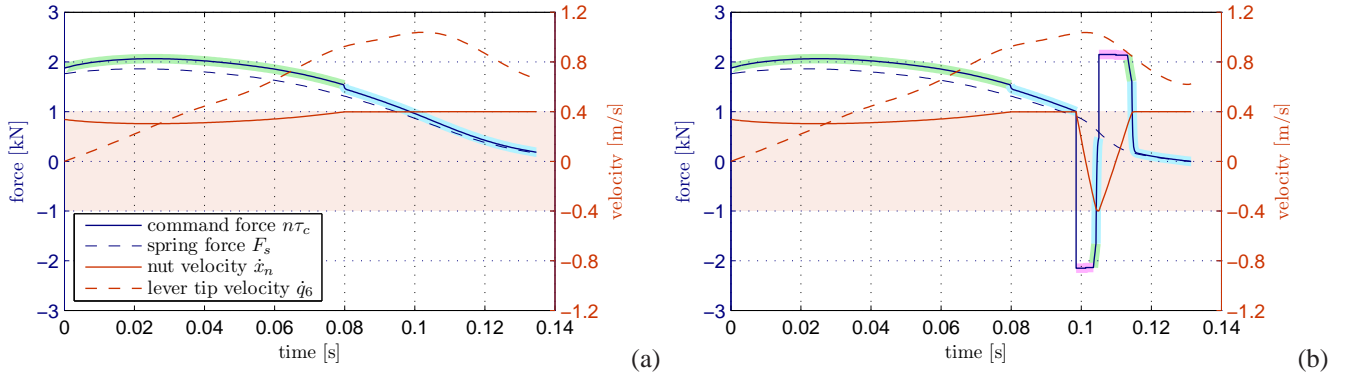
Fig. 7. Force and velocity results of a launch phase with (a) maximum positive steering and (b) steering to $p_f = 0$ using bang-bang control. The motor command torque τ_c is scaled with the transmission ratio of the ballscrew $n = 2\pi/0.004$ to obtain the equivalent command force. The type of command torque saturation is indicated by coloured highlights: voltage saturation in green, current saturation in purple, and speed saturation in cyan. The range of permissible nut speeds is shaded in pale orange.
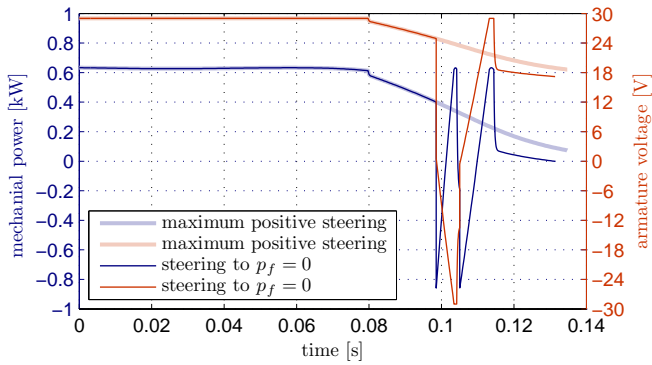

Fig. 8. Mechanical power and voltage for two steering actions. The motor is delivering maximum power (ca. 630 W) during most of the thrust phase due to maximum voltage (29 V) and optimal shaft velocity.

Fig. 10. The energy audit of Skippy's launch, where Skippy is performing negative steering towards $p_f = 0$. In comparison to the positive steering launch, it can be seen that slightly more energy is converted to heat.
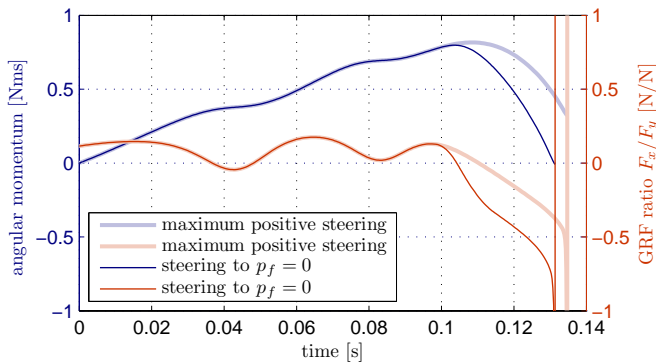

Fig. 9. Angular momentum build-up and GRF ratio for two steering actions. No slip occurs.

Figure 6 shows that nearly all of the spring energy (of which most from the main spring) is desirably converted to translational kinetic and gravitational potential energy, and that relatively little is converted to rotational kinetic energy. Most of the energy loss is 'motor heat', which is joule heating of the motor windings. Energy losses from the main spring and ballscrew add up to approximately 11 J. There is no regenerative heat loss in this particular graph because the motor is always performing positive mechanical work.
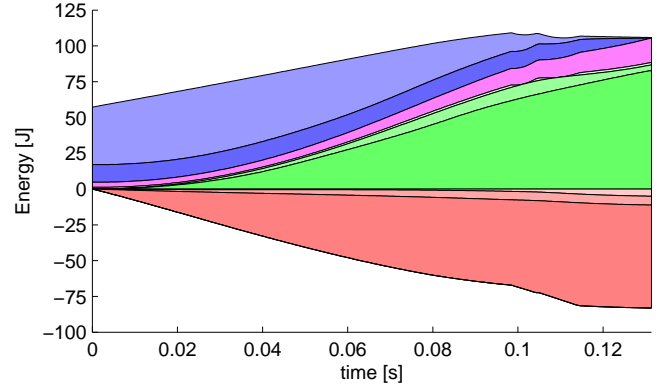
It can be seen in Figure 7 that the motor has been operating in saturation primarily due to voltage and secondarily due to nut speed, the latter reaching its maximum permissible speed at $t = 0.08$ s. While the motor is operating in saturation due to voltage, the motor is delivering close to maximum power because it is operating around ω_{opt}. The lever tip however is reaching a much higher velocity, which is due to the spring. A power drop can be observed in Figure 8 due to the voltage drop that is required when the nut reaches its maximum speed.

In Figure 9 it can be seen that angular momentum first builds up steadily, and then drops to about half its peak value during the final part of the motion. This is due to the unloading of the ankle, which changes the direction of the GRF. As the angular momentum does not drop to zero, Skippy will be making a backward somersault. In order to steer to zero momentum, a steering action is required, which can be accomplished by sending a different command torque to the motor during the steering phase.

After much experimentation, it was decided that it is not feasible to perform significant steering in the last few

moments before lift-off, because there is not enough time for these actions to have an effect. So most of the steering has to be done at the beginning of the steering phase. Provided that one can make a reasonable approximation at the beginning of the steering phase of lift-off time t_f and angular momentum $p_{f,max}$ for maximum positive steering (i.e., the result in Figure 9), we can perform an accurate steering action at the beginning of the steering phase that drives the lift-off momentum to a desired value, using the observation that there is a nearly linear relationship between a change of nut position Δx_n at the beginning of the steering phase integrated over time until lift-off and a change of lift-off momentum Δp_f, both changes being measured relative to the values that occur in the maximum positive steering case. Thus, we have that

$$p_f \approx \tilde{p}_f = \tilde{p}_{f,max} - \Delta \tilde{p}_f = \tilde{p}_{f,max} - c_s \left(\tilde{t}_f - t\right) \Delta x_n$$

where the gain c_s is obtained empirically, and $\sim$ indicates prediction. More generalized versions of this control strategy can be developed by allowing a continuous update of the estimated lift-off time and momentum throughout the steering phase, and by including the dynamic model into predictions and gain determination. However, for the purposes of demonstrating the physical possibility of steering, it was sufficient to implement a bang-bang controller in which the steering action consisted of a single pulse of deceleration torque command of sufficient magnitude to cause saturation, beginning at the start of the steering phase, and having a duration calculated to produce the desired value of Δx_n computed from the above equation. The beginning of the steering phase is currently defined by a fixed angle of the hip, at $q_3 + q_4 = 80°$, which is shortly before the ankle starts unloading for stance phases that aim for a 4 m high hop. This angle is reached at approximately $t = 0.1\,\text{s}$.

The results of a steering action that drive p_f to zero are displayed in Figures 7 to 10. The bang-bang controller requires the motor to do a tiny bit of negative work instead of positive work (the total regenerative heat is 0.1 J), and causes the motor to operate in current saturation, as can be seen in 7. The reduction in motor power output results in a slightly reduced jumping height, which is now 4.2 m. Since negative steering leads to a greater x-component of the GRF, the robot is more prone to slipping. However, it can be seen from Figure 9 that the robot does not slip for either steering action until the very last 0.4 ms[†].

B. Stance Phase

With a set of system parameters and initial conditions of the thrust phase that lead to a successful launch phase, the problem of generating a successful stance phase is simplified. The purpose of this section is to demonstrate the physical possibility of the action, and not to present a functional feedback control system. To do so, we adopt a simple feedforward strategy during the landing phase, identical to

[†]Slipping is assumed when the GRF goes outside a friction cone with an apex angle of 90°.

the one that has been used during the thrust phase: having the motor operate in saturation. The objective is then simplified to finding suitable initial conditions (as a result from the impact of the previous hop) that lead to a state of the robot that is approximately equal to the initial conditions of the thrust phase, and subsequently lead to satisfactory lift-off conditions.

The initial joint velocity conditions shortly after impact are calculated from Newton's inelastic impact law, based on Skippy's flight conditions shortly before impact. If we assume that all joint velocities are zero shortly before landing, and that both springs are relaxed, then the landing conditions can be described by only five independent state variables. These include three velocity terms and two position terms: the speed and direction of impact, v_{im} and α_{im}, the angular velocity of the robot before impact, ω_{im}, the angle of the CoM relative to the foot, β_0, and the hip angle, $q_{4,0}$.

v_{im} was tuned to obtain a desired impact velocity that leads to a 4 m hop. An initial estimate was based on obtaining a desired potential energy level of the main spring at initiation of the thrust phase—measured at the minimum crouching posture defined by the hip $q_{4,min}$—but was later increased to $v_{im} = 5.6\,m/s$ (corresponding to a previous vertical jump height of 1.6 m). $q_{4,0} = 20°$ was then selected based on a desired minimum crouching posture of $q_{4,min} \approx 5°$. α_{im}, ω_{im} and β_0 were found to obtain a desired lift-off direction and proper loading of the ankle, at $\alpha_{im} = 67.5°$, $\omega_{im} = 0\,\text{rad/s}$ and $\beta_0 = 106.8°$. Other sets of initial conditions also work.

Figures 11 and 12 display the results of a simulation with a steering action to $p_f = 0$, leading to a jump of 4.0 m. The main spring energy at initiation of the thrust phase is 52 J, which suggests a higher hopping height when compared to the results of the launch phase studies. The nut is subject to a higher force, which leads to current saturation during part of the thrust phase and reduces the motor power output. The relatively higher amount of heat developed in the system, as can be seen in Figure 11, is also an indication that high currents are drawn. Nonetheless, we have demonstrated the possibility of reaching a hopping height of 4 m by relying on less than half the required energy from the previous hop. A better control strategy would probably produce a more energy-efficient hop.

In Figure 12 it can be seen that Skippy would theoretically slip for the first few milliseconds, despite the near-vertical landing. This can be explained by the fact that the foot is more compliant at landing in the horizontal than in the vertical direction. Optimizing for system parameters of the ankle and initial conditions might solve the problem, and a slightly compliant rubber foot in reality might help as well.

VI. CONCLUSION

We have presented a design study leading to a hopping robot that hops 4 m high. In solving the problem of reaching a 4 m hop, we work within the capabilities of the system towards the end result, rather than imposing artificial dynamics on the robot by working back from a specified motion
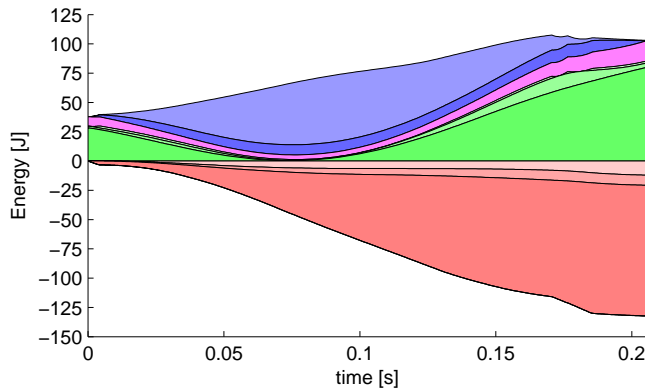
Fig. 11. The energy audit of Skippy's full thrust phase, where Skippy is performing negative steering towards $p_f = 0$.
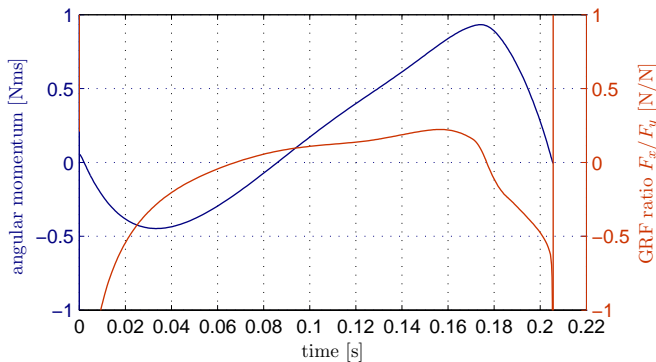

Fig. 12. Angular momentum and GRF ratio for the full stance phase leading to a $4\,\mathrm{m}$ hop.

to a desired torque command. The motor is operating in saturation and delivering close to maximum power, while the system's natural dynamics convert the resulting energy to useful kinetic energy for jumping. The resulting performance is close to what is physically maximally possible to achieve. In addition, we have shown that it is possible to use only one motor for generating vertical momentum (thrusting) and controlling rotational momentum (steering). A simulation of the full stance phase has further supported the theory. Whereas most parameters have been chosen through processes of reasoning, optimization studies could be done to further improve the results and tackle the trade-off between hopping and steering performance.

REFERENCES

[1] R. Armour, K. Paskins, A. Bowyer, J. Vincent, and W. Megill, "Jumping robots: a biomimetic solution to locomotion across rough terrain," *Bioinspiration & Biomimetics*, vol. 2, pp. S65–S82, 2007.

[2] M. F. Ashby, *Materials selection in mechanical design*. Pergamon Press, Oxford, 1992.

[3] M. Azad, "Balancing and hopping motion control algorithms for an under-actuated robot," Ph.D. dissertation, The Australian National University, June 2014.

[4] M. Azad and R. Featherstone, "Balancing and hopping motion of a planar hopper with one actuator," in *IEEE International Conference on Robotics and Automation*, 2013.

[5] ——, "Balancing control algorithm for a 3D under-actuated robot," in *IEEE/RSJ International Conference on Intelligent Robots and Systems*, 2014.

[6] M. Berg, "A non-linear rubber spring model for rail vehicle dynamics analysis," *Vehicle System Dynamics*, vol. 30, pp. 197–212, 1998.

[7] Boston Dynamics, *SandFlea – Jumping Robot (datasheet v1.0)*, 2012, accessed 25/02/2017. [Online]. Available: http://www.bostondynamics.com/img/SandFlea%20Datasheet%20v1_0.pdf

[8] J. J. M. Driessen, "Machine and behaviour co-design of a powerful minimally actuated hopping robot," Master's thesis, TU Delft, October 2015.

[9] R. Featherstone, "The Skippy Project," http://royfeatherstone.org/skippy/, February 2017, accessed 26/02/2017.

[10] ——, "Quantitative measures of a robot's physical ability to balance," *The International Journal of Robotics Research*, vol. 35, no. 14, pp. 1681–1696, September 2016.

[11] Festo, *Bionic Kangaroo (brochure)*, 2014, accessed 15/09/2016. [Online]. Available: https://www.festo.com/net/SupportPortal/Files/334103/Festo_BionicKangaroo_en.pdf

[12] D. W. Haldane, M. Plecnik, J. K. Yim, and R. S. Fearing, "A power modulating leg mechanism for monopedal hopping," in *International Conference on Intelligent Robots and Systems (IROS)*, 2016.

[13] G. P. Jung, C. S. Casarez, S. P. Jung, R. S. Fearing, and K. J. Cho, "An integrated jumping-crawling robot using height-adjustable jumping module," in *IEEE International Conference on Robotics and Automation*, 2016, pp. 4680–4685.

[14] F. Karlsson and A. Persson, "Modeling non-linear dynamics of rubber bushings - parameter identification and validation," Master's thesis, Lund University (Structural Mechanics), 2003.

[15] M. Kovač, M. Schlegel, J. C. Zufferey, and D. Floreano, "Steerable miniature jumping robot," *Autonomous Robots*, vol. 28, no. 3, pp. 295–306, 2009.

[16] T. McGeer, "Passive dynamic walking," *The International Journal of Robotics Research*, vol. 9, no. 2, pp. 62–82, April 1990.

[17] S. O'Sullivan, R. Nagle, J. A. McEwen, and V. Casey, "Elastomer rubbers as deflection elements in pressure sensors: investigation of properties using a custom designed programmable elastomer test rig," *Journal of Physics D: Applied Physics*, vol. 36, pp. 1910–1916, 2003.

[18] Pololu – Robotics & Electronics, "Pololu G2 high-power motor driver 24v21," https://www.pololu.com/product/2995, March 2016, accessed 25/02/2017.

[19] M. H. Raibert, *Legged Robots that Balance*. MIT Press,Cambridge, Massachusetts, 1986.

[20] W. J. Schwind and D. E. Koditschek, "Characterization of monoped equilibrium gaits," in *International Conference on Robotics and Automation*, vol. 3, 1997, pp. 1986–1992.

[21] S. Seok, A. Wang, M. Y. Chuah, D. J. Hyun, J. Lee, D. M. Otten, and J. H. Lang, "Design principles for energy-efficient legged locomotion and implementation on the MIT Cheetah robot," *IEEE/ASME Transactions on Mechatronics*, vol. 20, no. 3, pp. 1117–1129, June 2015.

[22] A. Seyfarth, H. Geyer, M. Günther, and R. Blickhan, "A movement criterion for running," *Journal of Biomechanics*, vol. 35, pp. 649–655, 2002.

[23] Steinmeyer, "Rolled ball screws - the alternative in linear technology," 2015, catalog.

[24] L. R. G. Treloar, "The elasticity and related properties of rubbers," *Reports on Progress in Physics*, vol. 36, pp. 755–826, 1973.

[25] M. A. Woodward and M. Sitti, "MultiMo-Bat: a biologically inspired integrated jumping-gliding robot," *International Journal of Robotics Research*, vol. 33, no. 12, pp. 1511–1529, 2014.

[26] V. Zaitsev, O. Gvirsman, A. Ben Hanan, U.and Weiss, A. Ayali, and G. Kosa, "Locust-inspired miniature jumping robot," in *IEEE International Conference on Intelligent Robots and Systems*, 2015.